Drug Deliv. and Transl. Res. (2015) 5:407–423
DOI 10.1007/s13346-015-0241-3

RESEARCH ARTICLE

Enhanced skin delivery of vismodegib by microneedle treatment

Hiep X. Nguyen [1] · **Ajay K. Banga** [1]

Published online: 12 June 2015

Abstract The present study investigated the effects of microneedle treatment (maltose microneedles, Admin Pen™ 1200, and Admin Pen™ 1500) on in vitro transdermal delivery of vismodegib with different needle lengths, skin equilibration times, and microneedle insertion durations. The influence of microneedle treatment on the dimensions of microchannels (dye binding, calcein imaging, histology, and confocal microscopy studies), transepidermal water loss, and skin permeability of vismodegib was also evaluated. Skin viscoelasticity was assessed using a rheometer, and microneedle geometry was characterized by scanning electron microscopy. Permeation studies of vismodegib through dermatomed porcine ear skin were conducted using vertical Franz diffusion cells. Skin irritation potential of vismodegib formulation was assessed using an in vitro reconstructed human epidermis model. Results of the in vitro permeation studies revealed significant enhancement in permeation of vismodegib through microneedle-treated skin. As the needle length increased from 500 to 1100 and 1400 μm, drug delivery increased from 14.50 ±2.35 to 32.38±3.33 and 74.40±15.86 μg/cm^2, respectively. Positive correlation between drug permeability and microneedle treatment duration was observed. The equilibration time was also found to affect the delivery of vismodegib. Thus, changes in microneedle length, equilibration time, and duration of treatment altered transdermal delivery of vismodegib.

✉ Ajay K. Banga
Banga_ak@mercer.edu

[1] Department of Pharmaceutical Sciences, College of Pharmacy, Mercer University, Atlanta, GA 30341, USA

Keywords Characterization · Skin irritation test · Microneedles · Transdermal delivery · Vismodegib

Abbreviations

BCC	Basal cell carcinoma
TEWL	Transepidermal water loss
SEM	Scanning electron microscopy
PBS	Phosphate-buffered saline
PEG 400	Polyethylene glycol 400
PG	Propylene glycol
SD	Standard deviation
HPLC	High-performance liquid chromatography
SIT	Skin irritation test
PPI	Pore permeability index

Introduction

Among more than two million cases of non-melanoma skin cancer diagnosed in 2006, approximately 80 % were basal cell carcinoma (BCC), which was reported as the most commonly occurring human skin malignancy [1, 2]. According to the American Cancer Society Facts and Figures 2013, 2.2 out of 3.5 million non-melanoma skin cancer cases that were treated annually in the USA were basal cell carcinoma. Advanced or metastatic BCC is an invasive form of disease which spreads distantly in the body and cannot be treated by surgery or radiation therapy [1]. Cancer cell growth in BCC occurs due to mutation in Smoothened, a transmembrane protein in Hedgehog signal transduction, which regulates the Hedgehog (Hh) pathway. Vismodegib (Hedgehog antagonist GDC-0449) was recently approved by US Food and Drug Administration to be a first-in-class, orally bioavailable inhibitor of Smoothened for use in patients with locally advanced

or metastatic BCC [1, 2]. Vismodegib electively deactivates the Hedgehog pathway by inhibiting the Smoothened protein, resulting in suppression of Gli-1/2 transcriptional activation that interferes with tumor cell growth and survival [1]. Presently, vismodegib is commercially marketed by Genentech as Erivedge™ capsule 150 mg. Vismodegib has a low oral absolute bioavailability (31.8 %), partly due to its poor water solubility (pH dependent with 0.1 μg/ml at pH 7) [3]. However, small molecular weight (421.30 g/mol), moderate lipophilicity (log P=2.7), and high permeability of vismodegib make it an ideal candidate for transdermal delivery. Furthermore, high plasma protein binding (greater than 99 %) facilitates diffusion of vismodegib through convective blood and lymphatic and interstitial transport into deep tissues [4].

Transdermal delivery is a promising and attractive route for delivering both small molecules and macromolecules [5–8] because of skin's large surface area, ease of use [7], patient compliance [8], and therapeutic effects. Transdermal delivery bypasses first-pass hepatic metabolism and, hence, is preferred for drugs with poor absorption rate and drugs which are unstable in the acidic environment of stomach or cause gastrointestinal tract irritation [7–9]. Another advantage of transdermal route is its ability to control the rate of drug delivery [8]. This can be explained by skin's extremely low permeability [5] rendered by the outermost lipophilic layer of dead corneocytes or the stratum corneum embedded in lipid-enriched matrix [10]. It is the greatest barrier and a key factor in regulating drug flux through the skin [5, 6]. The cellular, viable, avascular epidermis also offers a significant permeability barrier to the transport of drugs [6]. Successful transdermal delivery allows sufficient amount of drug to be transported across the epidermis to the superficial dermal capillary bed [6, 11]. Passive diffusion is traditionally limited to molecules of high potency (dose in milligrams or less), low molecular weight (<500 Da), and high-to-moderate lipophilicities [12]. Transdermal drug delivery can be enhanced by optimization of the drug formulation [8] or disruption of the skin barrier using chemical penetration enhancers [13] or physical approaches including lasers, electrical energy, ultrasound, radio frequency, and thermal energy [8, 14, 15].

Micron-size microneedles expand the scope of transdermal delivery by creating microscopic channels that enhance the delivery of therapeutic agents ranging in size from small molecules (including drug-loaded nanoparticles) to macromolecules such as proteins across the skin [5, 16]. Small and very sharp microneedles have sufficient length and strength to penetrate the stratum corneum and epidermis but do not stimulate the nerve fibers and blood vessels [5, 6]. Microneedles, due to their cost-effectiveness, ease of self-administration, and being minimally invasive, provide patient compliance [9]. As compared to transdermal patches, microneedles can deliver therapeutic amounts of pharmaceutical drugs in a shorter period of time [17]. Molecules can be placed at a desired depth in the skin [5] with relatively low microbial ingress [18] using needles of various lengths. Increase in microneedle density, insertion time, length, number of applications [19, 20], and force of insertion [21] have been reported to increase the in vitro diffusion rate of drugs across the skin. Microneedle treatment significantly enhanced the transdermal delivery of PEGylated naltrexone prodrug [22], nanoencapsulated dye [23], verapamil hydrochloride and amlodipine [19], and mannitol [11].

In the present study, maltose microneedles, Admin Pen™ 1200, and Admin Pen™ 1500 (Fig. 1) were used to enhance the in vitro penetration of vismodegib across dermatomed porcine ear skin. The studies included characterization of dermatomed porcine ear skin samples (dynamic viscoelasticity), microneedle dimensions, (scanning electron microscopy), and microchannels (dye binding studies, calcein imaging, histology, and confocal microscopy studies); investigation of skin after microneedle insertion (transepidermal water loss measurement); evaluation of transdermal drug delivery (in vitro permeation studies using vertical Franz diffusion cells and skin deposition studies); and acceptability of formulation for application (skin irritation test). The present study for the first time characterized microneedle geometry and dimensions of Admin Pen™ 1200 and Admin Pen™ 1500, measured depth and pore uniformity of microchannels in the skin created by Admin Pen™ 1200 and Admin Pen™ 1500, investigated the change of needle length and base dimensions of maltose microneedles after different treatment durations, studied dynamic viscoelastic properties of untreated and microneedle-treated dermatomed porcine ear skin using a rheometer, employed ImageJ to measure the surface area of microchannels to calculate the total surface area of pores

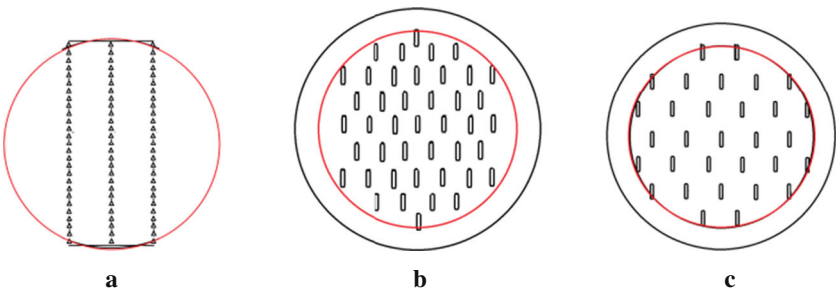

Fig. 1 Microneedle array on the in vitro diffusion area (0.64 cm^2, *red circle*). **a** Maltose microneedles, **b** Admin Pen™ 1200, **c** Admin Pen™ 1500

formed using different microneedles, and evaluated the skin irritation potential of vismodegib solution in propylene glycol (7 mg/ml). The study also investigated the effect of needle length (500, 1100, and 1400 μm), 30-min post-microneedle treatment equilibration time, and microneedle insertion duration (1, 2, and 4 min) on transdermal delivery of vismodegib.

Materials and methods

Materials

Vismodegib (GDC-0449) was purchased from MedChem Express LLC (Princeton, NJ, USA). Propylene glycol (PG), 0.1 M phosphate-buffered saline (PBS), and polyethylene glycol 400 (PEG 400) were obtained from Sigma-Aldrich (St. Louis, MO, USA), Fisher BioReagents, and Fisher Scientific (Fair Lawn, NJ, USA), respectively. Porcine ear skin was harvested in a local slaughterhouse (Atlanta, GA, USA). Fluoresoft® (0.35 %) was procured from Holles Laboratories, Inc. (Cohasset, MA, USA), and methylene blue dye from Eastman Kodak Co. (Rochester, NY, USA), while all the other chemicals were obtained from Sigma-Aldrich (St. Louis, MO, USA). Plates, assay medium, chemicals, nylon mesh, and other materials for in vitro skin irritation test were provided by MatTek Corporation (Ashland, MA, USA).

Maltose microneedles purchased from Elegaphy, Inc. (Tokyo, Japan) were solid, 500 μm in length, sharp tipped, and tetrahedron shaped. Each array included 3 straight parallel lines of 27 identical microneedles. Microneedle array-based pen injector devices, Admin Pen™ 1200 and Admin Pen™ 1500 metal microneedles, contained 43 and 31 microneedles, each 1100 and 1400 μm in length, respectively, and distributed as a diamond shape on a 1-cm^2 circular area (AdminMed, Sunnyvale, CA, USA) [24].

Methods

Scanning electron microscopy studies

The Phenom™ field emission scanning electron microscopy (SEM) system (Nanoscience Instruments, Inc., Phoenix, AZ, USA) and the Denton Vacuum Desk V sputter coater with gold target (Denton Vacuum LLC, Moorestown, NJ, USA) were utilized to investigate the microneedle shape, dimensions, surface morphology, and needle distribution pattern on array. Dust-free microneedles were placed in the field emission SEM at a primary beam-accelerating voltage of 5 kV to collect secondary ion images of different magnifications. A single line of maltose microneedle was carefully isolated from the array and mounted on SEM Pin stub mount (Ted Pella, Inc., Redding, CA, USA). Metal microneedle array was separated from Admin Pen™ 1200 and Admin Pen™ 1500 microneedle liquid injection system, stuck into low profile 45°/90° SEM mount (Ted Pella, Inc., Redding, CA, USA) using a double-sided carbon sticky tape, and sputter coated using a Denton Vacuum Desk V sputtering system with gold target in order to form a thin layer of conductive coating to increase the signal-to-noise ratio. SEM images were analyzed to obtain the dimensions of microneedles such as needle length, base size, and tip-to-tip distance. After different microneedle treatment durations (1, 2, and 4 min), an individual line of maltose microneedle was separated for SEM analysis to investigate the change in needle length and base dimensions.

Preparation of skin samples

Freshly excised porcine ear skin obtained from the local slaughter house was washed with 10 mM PBS, wrapped in aluminum foil, and stored at −80 °C. In order to obtain a relatively uniform skin thickness, specific sections of the ears were processed according to the study of Han et al. [25]. The stored skin was thawed at room temperature for 30 min. After being completely thawed, the full-thickness porcine ear skin was washed with 10 mM PBS solution and dermatomed to an average thickness of 0.60±0.11 mm (n=40) (measured using a digital micrometer, Marathon Watch, 1.55 V) using a Padgett electro-dermatome (Kansas City Assemblage Co., Kansas City, MO, USA) after trimming the hair. Then, the skin was cut into 2×2 cm^2 pieces for the study.

Dynamic viscoelasticity properties of porcine ear skin

Exploring the effect of microneedle treatment on drug delivery gets more complicated and challenging due to the viscoelastic nature of skin [20]. The importance of considering skin viscoelasticity during microneedle insertion has been reported in the literature [26]. In the present study, the viscoelasticity of freshly dermatomed porcine ear skin and microneedle-treated skin was evaluated using an oscillatory rheometer (Rheoplus/32 V3.62; Anton Paar Germany GmbH, Germany). Skin samples were kept static on the plate during the test with the normal force of 2–3 N. The storage modulus and loss modulus of the skin were studied at a constant volume strain of 1 % with an increasing angular frequency from 6 to 474 rad/s at 32 °C to simulate the skin surface temperature and reduce the thermal effects on the test results. The storage modulus (G') depicts stored energy or elastic properties, while the loss modulus (G'') demonstrates the energy dissipated as heat or viscous properties of the material. If G' is high, the skin will be more resistant to the external forces during microneedle insertion [21].

Dye binding studies

Methylene blue solution (1 % *w/v* in deionized water) was used to confirm the formation of microchannels in the skin [16]. The freshly dermatomed porcine ear skin with the stratum corneum towards the top was placed flat on four layers of parafilm (Parafilm M Laboratory film; Neenah, WI, USA) to mimic the soft tissue under the skin and avoid microneedle breakage. The center of skin (desired treatment site) was stretched with fingers before manually inserting the microneedles by thumb with a relatively uniform force of approximately 40 N (confirmed by a balance). The Admin Pen™ was mounted on commercially available 10-ml syringe prior to use. After inserting for 1 min in the skin, the microneedle array was removed. Methylene blue dye was immediately applied on the treated site for 1 min before being swabbed using Kimwipes (Kimberly-Clark Worldwide, Inc.) and alcohol swabs (alcohol prep, Curity™; Covidien, MA, USA) to remove excessive stain. The stained site was visualized using a ProScope HR Digital USB Microscope (Bodelin Technologies, OR, USA).

Histology studies

Histological sectioning was performed to assess the ability of microneedles to pierce dermatomed porcine ear skin and create microchannels. A small piece of skin (1×1 cm^2) was microporated, stained using 1 % (*w/v*) methylene blue solution, cleaned with Kimwipes and alcohol swabs after 1 min, and placed flat in Tissue-Tek® optical coherence tomography (OCT) compound medium (Sakura Finetek USA, Inc., Torrance, CA, USA). This block was solidified by storing under −80 °C for 1 h before sectioning using Microm HM 505 E (Southeast Scientific, Inc., GA, USA) with the section thickness of 10 μm. The block was tightly glued onto the object holder in the microtome chamber at −20 °C using an embedding medium. The sample was cut, and the cryosections of the skin samples were mounted on microscope glass slides (Globe Scientific, Inc., NJ, USA) and visualized using a Leica DM 750 microscope.

Confocal microscopy studies

The depth and surface area of microchannels created by microneedles were measured using confocal microscopy. Freshly dermatomed porcine ear skin was treated with maltose microneedles, Admin Pen™ 1200, or Admin Pen™ 1500. Fluoresoft® (0.35 %, 200 μl) was then applied for 1 min after which the excessive calcein was removed using Kimwipes and alcohol swabs. The treated skin was placed on a microscope slide without fixation artifacts or distortion and scanned using a computerized Leica SP8 confocal laser microscope (Switzerland) with ×10 objective at an excitation wavelength of 496 nm. Fluorescent images were then processed by Leica Application Suite-Advanced Fluorescence (LAS-AF) software. X-Z sectioning was employed to study the distribution pattern of calcein in the channels and the depth of the created microchannels. The surface area of micropores was calculated from the microscopic images using ImageJ 1.41o (National Institutes of Health, USA).

Pore uniformity studies

The uniformity of microchannels and relative flux values of individual channels were investigated by calcein imaging using Fluorophore image analysis tool. Fluoresoft® (0.35 %) solution was applied for 1 min on the microneedle-treated site of the skin and then wiped off with Kimwipes and alcohol swabs. The protocol has been described by Kolli and Banga [5]. A two-dimensional fluorescent image was taken to show the distribution of fluorescent intensity in and around each pore that was then converted into pore permeability index (PPI). The PPI value represented the calcein flux for each pore.

Transepidermal water loss measurement

The barrier integrity and humidity of porcine ear skin before and after microneedle treatment were evaluated rapidly and non-invasively by transepidermal water loss (TEWL) value measurement using a VapoMeter with a closed chamber (Delfin Technologies, Ltd., Kuopio, Finland). The probe was kept on the skin for 13 s to obtain the values on the screen (n=4). The TEWL studies depicted the effects of microneedle treatment on skin barrier function. Normal skin showed a small amount of water loss, while the water loss increased significantly as the skin barrier was disturbed [5]. In other words, an increase in TEWL value indicated compromised skin. The experiments were conducted to compare the TEWL values of different microneedle treatment groups.

In vitro permeation studies using vertical Franz diffusion cells

In vitro permeation study is a useful technique to measure the rate and extent of drug transported across the skin. In the present project, permeation studies of vismodegib through porcine ear skin were performed using jacketed PermeGear V6 station vertical Franz diffusion cells with 9 mm orifice and 0.64 cm^2 diffusion area (Hellertown, PA, USA). The objective of this study was to investigate the effects of needle length (500 μm of maltose microneedles, 1100 μm of Admin Pen™ 1200, and 1400 μm of Admin Pen™ 1500), skin equilibration time from piercing the skin with microneedles till applying the drug formulation (0 or 30 min), and treatment duration for which the microneedles were kept in the skin by

thumb (1, 2, or 4 min) on drug delivery across the skin. Donor chamber contained 100 μl of vismodegib solution in 7 mg/ml propylene glycol (90 % saturation level [27]) to give a dose of 1.1 mg/cm^2. The donor chamber was kept open to mimic in vivo conditions. The receptor compartment was filled with 5 ml of receptor solution (10 mM PBS/PEG 400, 50:50 *v*/*v*). Receptor was maintained at 37 °C using built-in water circulation jacket surrounding the lower part of the Franz cells to have the skin surface temperature of 32 °C. The receptor fluid was continuously, magnetically stirred during the studies. The procedure followed "poke and patch" mechanism where micropores were created by insertion and removal of the microneedles before the drug formulation was applied [19]. Microneedles were manually inserted at the desired skin treatment site and removed after 1 min in an identical protocol as in dye binding studies. The microporated skin was clamped between the donor and receptor chamber with the stratum corneum facing upwards. Air bubbles below the surface of the skin were eliminated carefully by tilting the cells. The transdermal delivery of vismodegib was measured by removing aliquots of 300 μl receptor fluid from sampling port using a 1-ml graduated plastic syringe at 0, 1, 2, 4, 6, 8, 10, 22, and 24 h, followed by replacement with an equal volume of fresh receptor solution to maintain a constant receptor volume. All samples were analyzed using a sensitive, specific, and reliable gradient reversed-phase high-performance liquid chromatography (HPLC) method with the linearity range of 0.1–50 μg/ml (R^2=1.000) and the limit of detection of 0.04 μg/ml [27]. The cumulative amount of vismodegib permeated through a diffusion unit area was plotted as a function of time (n=4).

Skin disposition studies

After 24 h of permeation studies, the skin was carefully cleaned three times with Q-tips soaked in 10 mM PBS/PEG 400 (50:50 *v*/*v*) and dabbed with Kimwipes to remove the donor formulation. In order to measure the drug levels in the skin, a tape-stripping technique was used to separate the stratum corneum from the epidermis and dermis. Adhesive tapes (3M transpore tapes; 3M Healthcare, St. Paul, MN, USA) were cut into pieces (1.9×1.9 cm^2). Twenty tapes were applied onto the permeated skin site one-by-one, pressed for proper adhesion, rolled with a glass rod, and removed quickly with forceps. Tapes 1–5, tapes 6–10, and tapes 11–20 were collected individually in six-well plates (Becton Dickinson, Franklin Lakes, NJ, USA). The remaining skin was manually minced with surgical scissors and placed in a separate six-well plate. Ethanol (2 ml) was added to each well. The wells were then placed on a shaker at 150 rpm for 4 h, and the samples were filtered through a 0.2-μm filter and analyzed using the HPLC method.

Skin irritation test

The in vitro EpiDerm™ skin irritation test (EPI-200-SIT) using the three-dimensional in vitro reconstructed human epidermal (RHE) model EpiDerm (MatTek Corporation, Ashland, MA, USA) is an effective method to classify drug formulation into either irritants of GHS category 2 or non-irritant [28, 29]. It was critical to understand whether vismodegib formulation (solution 7 mg/ml in propylene glycol) would alter the stratum corneum and cause irritation to the skin. The EpiDerm™ SIT has sufficient accuracy and reliability to be used as an in vitro replacement for animal skin irritation testing [28]. The present study is the first one that reports the skin irritation test data of the vismodegib formulation. Aqueous sodium dodecyl sulfate (SDS) solution (positive control), Dulbecco's phosphate-buffered saline (DPBS, negative control), and 30 μl vismodegib solution (test) were applied on separate skin tissues and kept for 60 min in an incubator (37±1 °C, 5±1 % CO_2, 95 % relative humidity (RH)). Three replicates of tissues were performed for each solution. The tissues were rinsed with DPBS before being transferred to fresh assay medium. The tissues were incubated for 24 h at 37±1 °C, 5±1 % CO_2, 95 % RH [28]. Incubation was continued for the next 18 h after replacing the medium with fresh one. Methyl thiazolyl tetrazolium (MTT) assay was then conducted by transferring the tissues into yellow MTT solution (1 mg/ml). After 3 h of incubation, the blue formazan salt formed by cellular mitochondria was extracted with 2 ml isopropanol. The optical density of the extracted formazan was measured using a spectrophotometer at 570 nm. Due to the long post-incubation period, the test was performed under aseptic conditions in a laminar flow hood. A chemical was classified as non-irritant if the mean relative tissue viability of three individual tissues was more than 50 % of the mean viability of the negative control [28, 29].

Data analysis

All results were reported as the mean with standard deviation (SD). Statistical calculations were performed in Microsoft Excel Worksheets and the SPSS software package version 21.0 (IBM, USA). The one-way ANOVA followed by Tukey's HSD post hoc test was used to compare the results of different groups. Statistically significant difference was depicted by p value <0.05.

Results and discussion

Scanning electron microscopy studies

The SEM images of small portions of microneedle arrays (Fig. 2) were magnified by different factors to study the

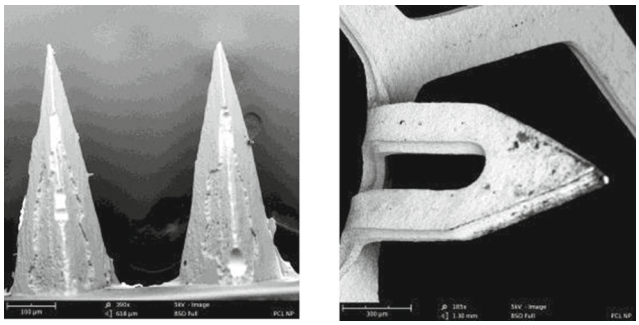

a b

Fig. 2 SEM image of **a** maltose microneedles and **b** Admin Pen™ 1500

morphology and dimensions of maltose microneedles, Admin Pen™ 1200, and Admin Pen™ 1500 (Table 1).

The results of microneedle dimensions were consistent with other research studies that characterized the pyramid-shaped solid maltose microneedles with a needle length of 508.46±9.32 μm [5] or 497.41±31.10 μm [16] and an equilateral triangle side of the base of 204.62±7.19 μm [5] or 197.60±17.53 μm [16]. The length of Admin Pen™ was in concordance with the information provided by AdminMed that Admin Pen™ 1200 and Admin Pen™ 1500 stainless steel microneedles were 1100 and 1400 μm in length, respectively [24]. All the parameters including needle density, height, base length, width, and needle-to-needle distance of Admin Pen™ 1200 and Admin Pen™ 1500 were similar to those of Admin Patch 1200 and Admin Patch 1500 [17, 21, 30]. The measured dimensions showed the likeliness of all the microneedles to pierce porcine ear skin having stratum corneum thickness of 21–26 μm and viable epidermis thickness of 66–72 μm [31].

As the treatment duration increased from 1 to 2 and 4 min, maltose microneedles gradually dissolved and their length decreased significantly from 179.70±64.54 μm (n=10) to 86.90 ±67.53 μm (n=10) (p<0.05) and 0 μm (p<0.05), respectively, but the length of the equilateral triangle side of the needle base showed an insignificant change from 252.30±25.23 to 261.20±43.71 μm (p=0.58). When the maltose microneedles were inserted in the skin for 4 min, the entire needles dissolved to give SEM images of only the substrate without any visible traces of microneedles.

Dynamic viscoelasticity properties of porcine ear skin

The difference in viscoelasticity of skin samples was observed to affect the insertion behavior of microneedles. Figure 3 shows the storage modulus (G') and loss modulus (G'') of untreated dermatomed porcine ear skin and microneedle-treated skin as a function of angular frequency (ω). Both G' and G'' increased with an increase in angular frequency. As seen in Fig. 3a, the storage modulus of untreated skin sample (>10,000 Pa) was determined to be greater than the loss modulus (around 2500 Pa) which indicated that dermatomed porcine ear skin would be more elastic and, hence, presents a high resistance to external force. Figure 3b, c shows that microneedle treatment reduced the storage modulus and loss modulus of the skin samples.

According to the results of skin dynamic viscoelasticity, full-thickness porcine ear skin was found to be more elastic with the storage modulus over 15,000 Pa and loss modulus around 5000 Pa [21, 30]. In other words, the dermatomed skin samples were less resistant to microneedle insertion force than full-thickness skin or a change in the thickness was found to alter the skin viscoelasticity. The reduction of storage modulus and loss modulus due to maltose microneedle, Admin Pen™ 1200, and Admin Pen™ 1500 treatment suggests that the skin samples became less viscoelastic and less resistant to external force after the treatment.

Dye binding studies

Dye binding studies were conducted to confirm the microneedles' ability in terms of sharpness, length, and density to pierce the stratum corneum and create micron-size channels in the skin. Methylene blue dye would bind to the successfully created microchannels and be visible under the ProScope HR Digital USB Microscope.

Table 1 Microneedle dimensions

Microneedle dimensions (μm)	SEM image magnification	Maltose microneedles	Admin Pen™ 1200	Admin Pen™ 1500
Length (n=10)	×400	505.90±9.54		
	×200		1108.30±21.81	1396±8.89
Tip-to-tip distance (n=10)	×400	353.30±13.82		
	×100		1638.60±10.15	2010.70±12.68
Base				
Shape		Equilateral triangle	Rectangle	Rectangle
Dimensions (n=10)	×400	223.70±13.16		
	×200		456.20±9.58 (long) 89.80±6.39 (wide)	562.90±9.00 (long) 120.40±9.28 (wide)

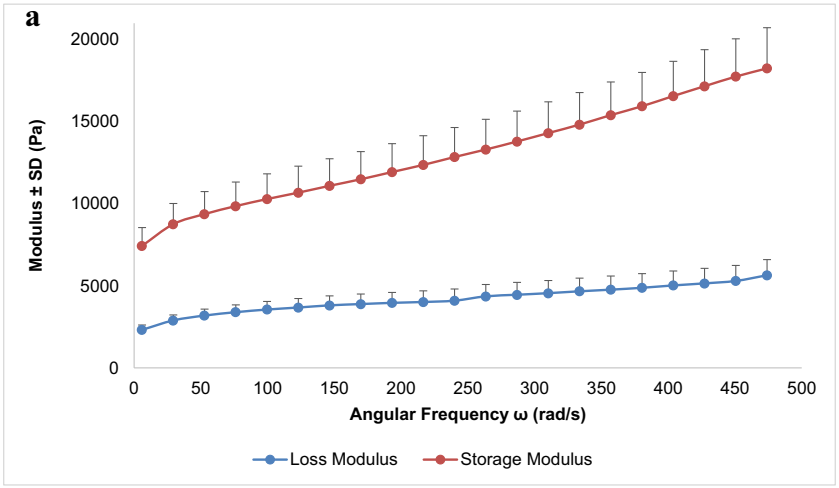

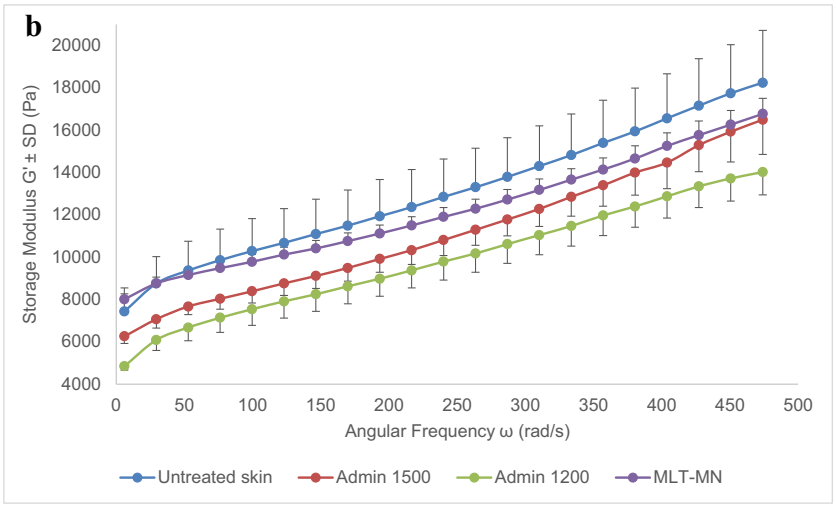

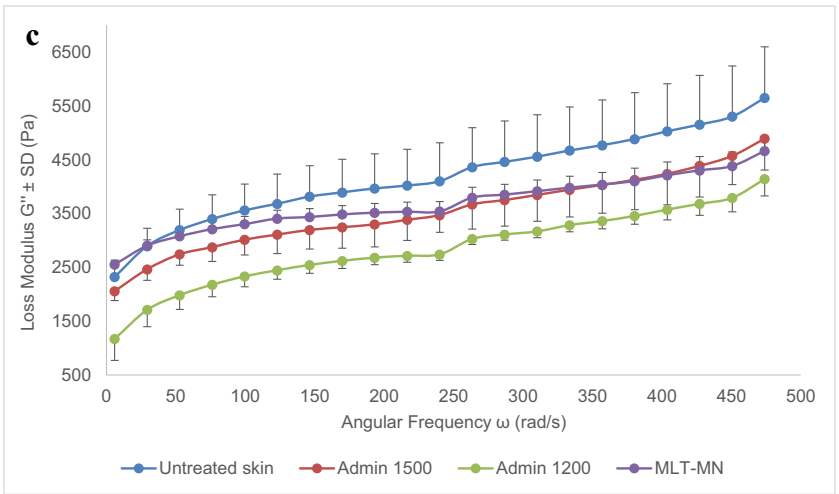

Fig. 3 **a** Dynamic viscoelastic properties of untreated dermatomed porcine ear skin. **b** Storage modulus of untreated dermatomed porcine ear skin and microneedle-treated skin. **c** Loss modulus of untreated dermatomed porcine ear skin and microneedle-treated skin. *Admin 1200* Admin Pen™ 1200, *Admin 1500* Admin Pen™ 1500, *MLT-MN* maltose microneedle

Magnified view of a small portion of microneedle-treated site showed that methylene blue dye diffused along the periphery of the microchannels into the lower epidermal tissue, however, did not stain other areas on the skin samples. Figure 4 represents several stained microspots on the skin with the distance between them in accordance with the tip-to-tip

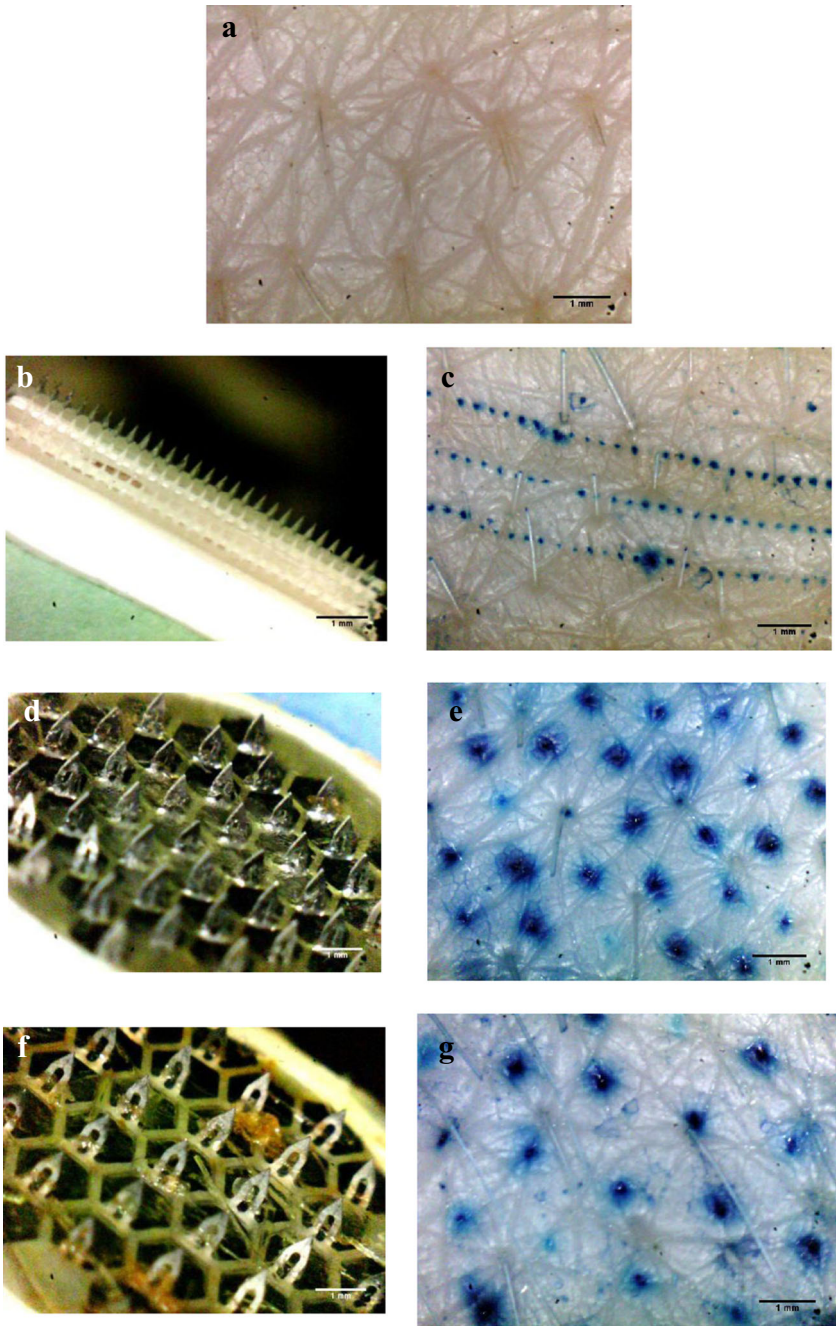

Fig. 4 Microchannels created in dermatomed porcine ear skin. **a** Untreated skin; **b**, **c** maltose microneedle array and the channels; **d**, **e** Admin Pen™ 1200 array and the channels; **f**, **g** Admin Pen™ 1500 array and the channels

distance of microneedles on arrays. This shows that the microchannels were created only by the microneedles. In other words, the substrate of maltose and Admin Pen™ microneedles did not disturb the barrier function of the stratum corneum. Hair follicles did not take up methylene blue and therefore did not show up by staining. As shown in Fig. 1, an array of maltose microneedles, Admin Pen™ 1200, and Admin Pen™ 1500 provided a pore density of 81, 43, and 31 pores/0.64 cm^2, respectively. These results were in agreement with the microneedle density on the array provided by Elegaphy and AdminMed [24]. The base of maltose microneedles was found not to have a significant effect on the stratum corneum barrier as also reported by Kolli and Banga [5]. The center-to-center distance between any two adjacent microchannels created by maltose microneedles within the same line and two adjacent lines was 370.74±41.42 and 1130.34±63.68 μm, respectively, while Admin Pen™ 1200 and Admin Pen™ 1500 formed microchannels that were 1650.71±109.33 and 2046.75±127.22 μm apart, respectively (n=5). These results were similar to our earlier study that used methylene dye binding studies for maltose microneedle treatment on full-thickness hairless rat skin and

reported the distance between two microchannels within the same line and two adjacent lines to be 376.38±14.37 and 1071.10±64.92 μm, respectively [5].

Histology studies

Vertical sectioning perpendicular to the surface of the skin was used to visualize 10-μm-thick cryosections of the microneedle-treated skin samples under a Leica DM 750 microscope with different magnifications. Moreover, histological sectioning images depicted the morphology of microchannels in the skin.

The vertical sections of the skin samples in Fig. 5 indicate that the cross section and shape of microchannels were consistent with the geometry of microneedles characterized by SEM studies. The pyramidal maltose microneedles created somewhat triangular sections, while Admin Pen™ provided nearly rectangle-shaped sections.

Confocal microscopy studies

The depth and surface area of microchannels were studied by Leica SP8 confocal laser microscopy without any dimensional distortions during physical sectioning.

Hair follicles did not show up in the confocal images (Fig. 6) which revealed that calcein did not transport through follicular pathway. As the micropores greatly differed in their shape, it was not advisable to measure the diameter of the pores in the treated skin. Instead, confocal images of micropores of various magnifications were analyzed by ImageJ software to calculate the surface area of the pores. The surface area of the pores formed by maltose microneedles, Admin Pen™ 1200, and Admin Pen™ 1500 was found to be 12018.01±2682.68 μm^2 (55.29 % of the average needle base area), 23681.45±2434.16 μm^2 (57.79 % of the average needle base area), and 47967.86±15315.1 μm^2 (70.77 % of the average needle base area), respectively. The results are presented as the mean pore surface area±SD (n=10). This observation could be co-related with the literature that reports the contraction of channels in a relatively short time after microneedle removal due to the inherent elasticity of the skin [16, 32].

The number of microchannels created on the diffusion area of skin samples multiplied with the surface area of each channel gave the total surface area of the microchannels created by each kind of microneedles (shown in Fig. 7).

Figure 7 illustrates that the total surface area of microchannels created by Admin Pen™ 1500 on the diffusion area was significantly greater than that created by maltose microneedles and Admin Pen™ 1200 ($p<0.05$). The surface area of microchannels needs to be considered for transport and potential infection considerations [18].

A z-stack was defined as a sequence of basic images captured at the same horizontal position (x, y) but at different imaging depths (z). The z-stack was conducted at different steps starting from the skin surface to the end of microchannels or the point where the signal of calcein visually disappeared. The step size of z-stack was either 5, 10, or 20 μm. The z-stack indicated the depth that the channels could reach in the dermatomed porcine ear skin as presented in Table 2. The results showed that an increase in needle length from 500 to 1100 and 1400 μm significantly enhanced the depth of the microchannels in the skin. As shown in Fig. 8, the intensity of calcein decreased along the microchannels.

Based on confocal microscopy images, the morphology of micropores followed the geometry of microneedle base on arrays. In particular, maltose microneedles created nearly triangular microchannels while oval-shaped channels were observed in confocal images of the skin samples treated with either Admin Pen™ 1200 or Admin Pen™ 1500. Similar findings where the surface morphology of the pores was observed to be noticeably close to the shape of the microneedles have been reported by other researchers [5]. The depth of microchannels in the present study was consistent with the statement of Martanto et al. that, typically, only 10–30 % of the microneedle length penetrated the tissue [33]. In other projects, the depth of the channels made by maltose microneedles was found to be 153.33±20.82 μm [16] or 160 μm [5]. A possible explanation for the lower penetration of microneedles was proposed that at first contact with the skin, part of the needles just indent the skin while the rest penetrates after a sufficient pressure is applied [33]. The depth of microchannels depended on the insertion pressure of microneedles, needle density, viscoelasticity, and integrity of

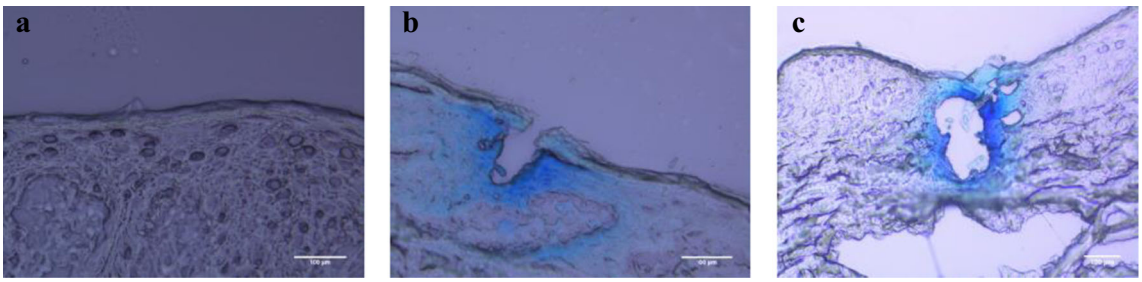

Fig. 5 Histological sectioning images of untreated skin (**a**) and those treated by maltose microneedles (**b**) or Admin Pen™ 1500 (**c**)

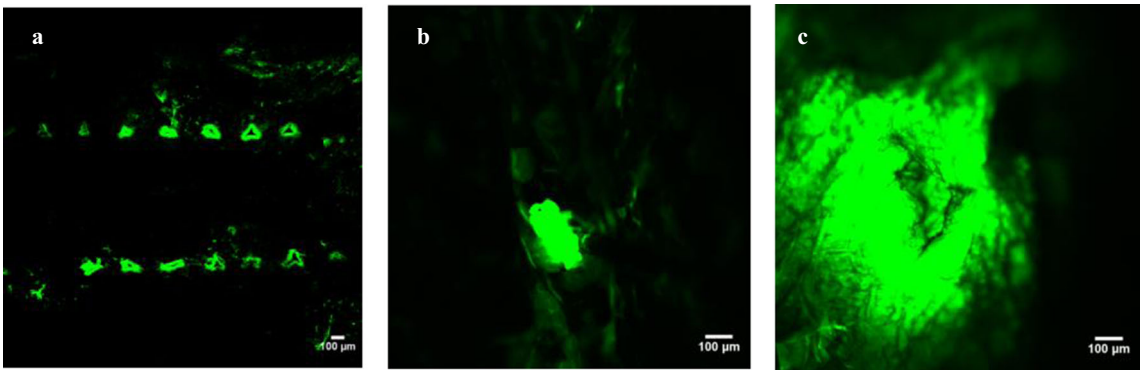

Fig. 6 Confocal images of skin samples treated with **a** maltose microneedles, **b** Admin Pen™ 1200, and **c** Admin Pen™ 1500

skin samples [34]. The stratum corneum of the human skin is 10–15 μm in thickness, while the thickness of epidermis is 50–100 μm [10]. Based on the depth of microchannels, microneedles would most likely reach the skin dermis.

Pore uniformity studies

The fluorescent images were analyzed by Fluorophore software for the volumetric distribution of calcein in and around each pore. The PPI is an accurate, reliable, and ratiometric indicator of the relative flux for each pore. As shown in Fig. 9, the average PPI values of pores created by maltose microneedles (70 pores) and Admin Pen™ 1200 (35 pores) and Admin Pen™ 1500 (29 pores) microneedles were 11.70±4.40, 32.1±21.61, and 63.90±27.12, respectively. One of the pores created by Admin Pen™ 1200 and Admin Pen™ 1500 was assigned zero PPI value, while all the channels created by maltose microneedles were included in the analysis.

The bell-shaped distribution pattern of the PPI histogram of pores created by maltose microneedles indicated the uniformity of the pores. This result was similar to that of our previous report that maltose microneedle arrays provided relatively uniform channels (average PPI values 2.30±1.27 for 79 pores) [5]. Besides, the pore uniformity studies also showed that the pores created by Admin Pen™ 1500 (63.90±27.12, n=29) were bigger and less uniform than those created by Admin Pen™ 1200 (32.1±21.61, n=35). This observation was also in agreement with the results of the dye binding and confocal studies as reported earlier.

Transepidermal water loss measurement

Prior to permeation experiments, the integrity of skin samples and the formation of microchannels were investigated by TEWL measurement studies [23]. The symbols of different skin treatment groups are elaborated in Table 3. The TEWL values of the skin with different microneedle treatment methods are shown in Fig. 10.

An increase in needle length from 500 μm (maltose microneedles) to 1100 μm (Admin Pen™ 1200) and 1400 μm (Admin Pen™ 1500) enhanced the TEWL values from 31.10±5.67 to 40.73±13.11 and 43.33±9.73 g/m^{2}h, respectively. This trend was consistent with the results of the depth and surface area of microchannels previously characterized by the confocal microscopy studies. In the present study, significantly higher TEWL values were found in the case of

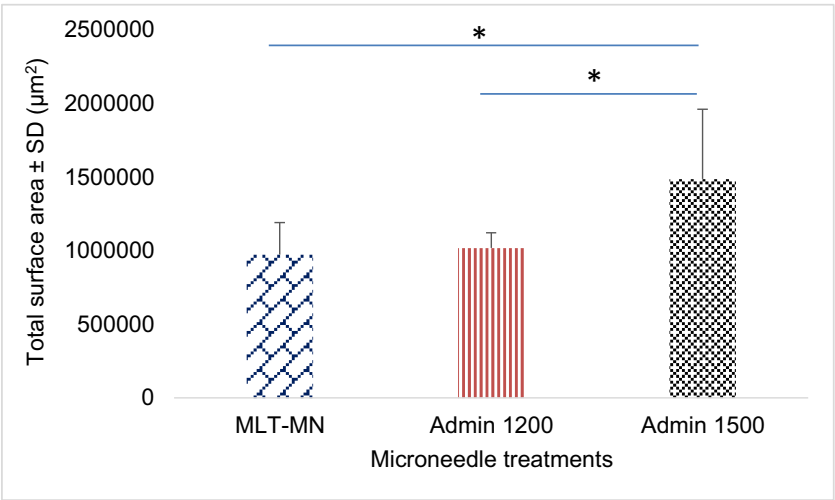

Fig. 7 The total surface area of microchannels created by microneedles (*asterisks* indicate the statistical difference from Admin 1500 and MLT-MN and Admin 1200 groups). *Admin 1200* Admin Pen™ 1200, *Admin 1500* Admin Pen™ 1500, *MLT-MN* maltose microneedle

Table 2 The average depth of microchannels

Microneedles	Depth of microchannels (μm) (n=10)
Maltose microneedles	140.5±10.12
Admin Pen™ 1200	242.5±22.27
Admin Pen™ 1500	278±33.35

Admin Pen™ 1200 (Admin 1200) (p=0.025) and Admin Pen™ 1500 (Admin 1500) (p=0.004) groups than the control group. Besides, 30-min equilibration time after maltose microneedle insertion (M3OE) increased the TEWL value to 33.50±5.44 g/m^{2}h. Similar results were observed by Gomaa et al. [20, 23] and Badran et al. [11] that as the equilibration time after microneedle treatment increased, the TEWL value first increased, reached the maximum level at 1 h, and then eventually decreased due to the closure of the micropores over time. However, there was no significant difference of TEWL values between groups of different treatment durations or of different kinds of microneedles (p>0.05). In the literature, microneedle insertion period of 3 or 5 min was found to produce similar TEWL plot [20]. The TEWL measurement concluding a positive correlation between TEWL values and microneedle length has also been reported in other researches [11, 35]. An increase in TEWL values due to microneedle treatment was an indicator that all microneedles used in the present experiments successfully disrupted the stratum corneum and integrity of the skin. This change was comparable to that already mentioned in the literature that the TEWL values of skin samples were enhanced sharply by microneedle insertion [16, 20, 22]. The basal TEWL value measured for control group was 20.93±2.68 g/m^{2}h. This value was similar to the reported values in other projects where Gomaa et al. estimated the TEWL value of untreated full-thickness porcine ear skin to be 29.40±2.60 g/m^{2}h [23] and Elmabjoubi et al. measured the basal TEWL value of about 35 g/m^{2}h [36].

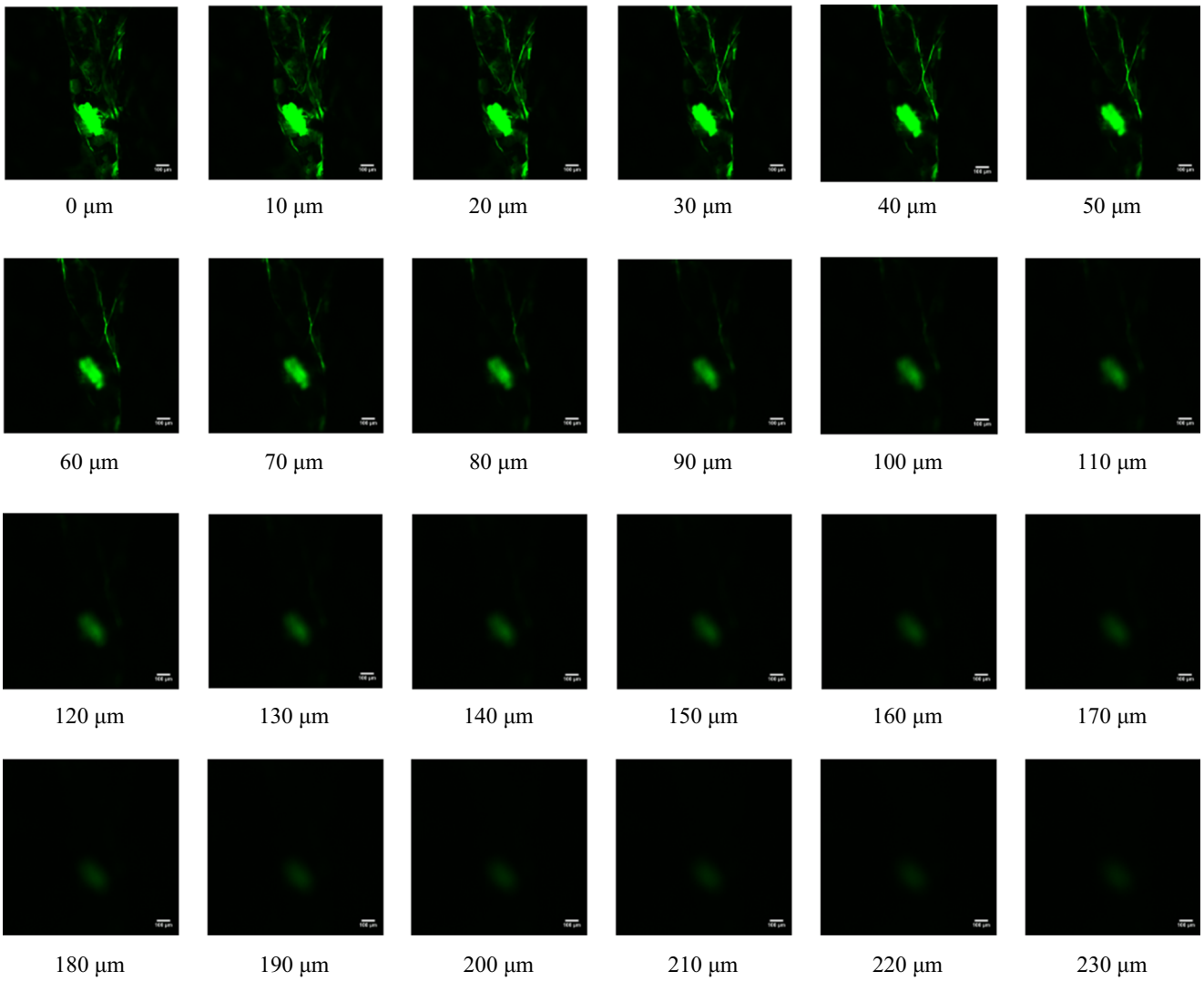

Fig. 8 Confocal microscopy z-stack of microchannels created by Admin Pen™ 1200

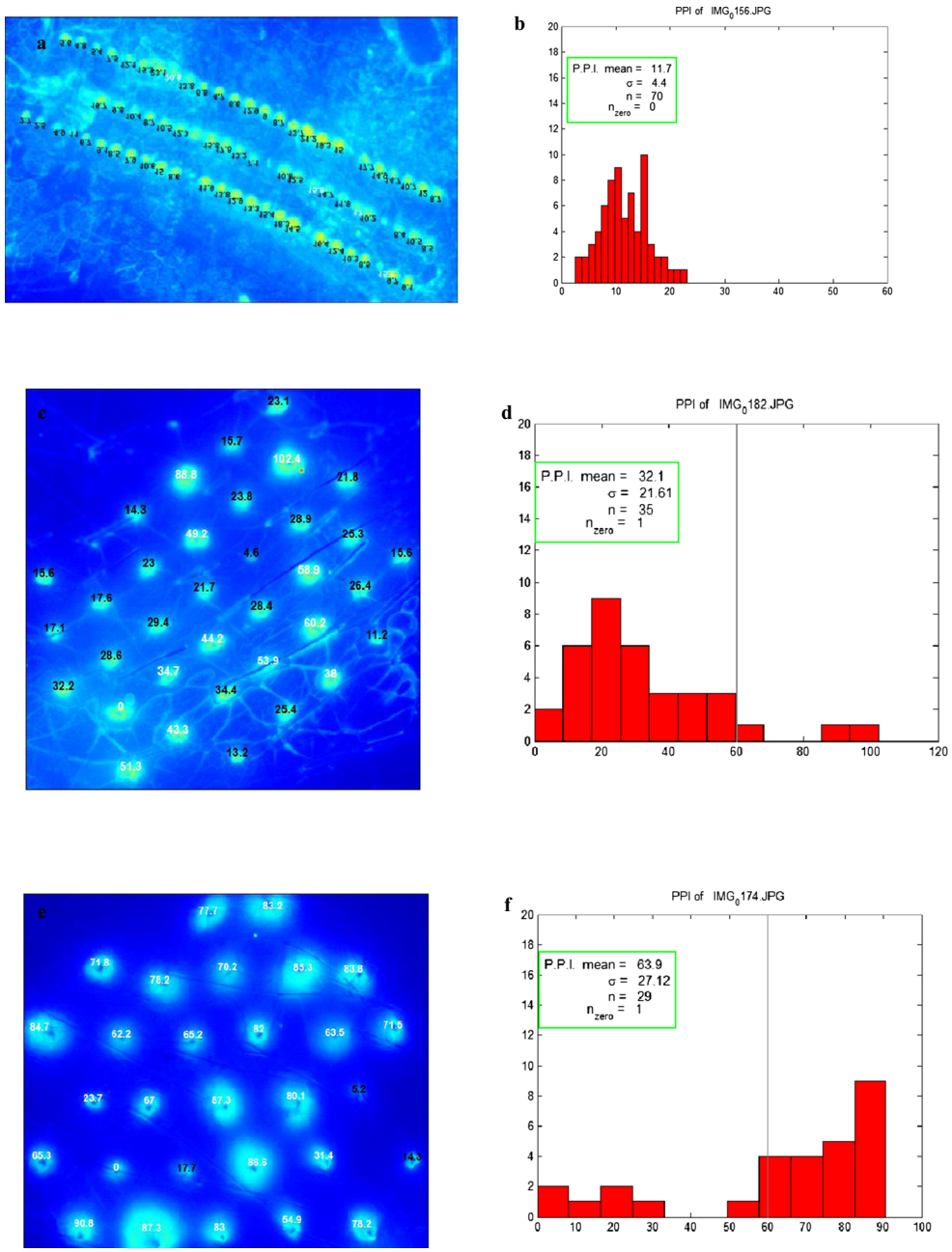

Fig. 9 The microchannels with pore permeability index (*PPI*) values and histogram of **a**, **b** maltose microneedles; **c**, **d** Admin Pen™ 1200; and **e**, **f** Admin Pen™ 1500

Table 3 Group symbols of different skin treatment methods

No.	Symbols	Dermatomed porcine ear skin treatments
1	Control	No microneedles, no equilibration
2	Control 30E	No microneedle treatment, 30-min equilibration
3	MLT-MN	Maltose microneedle treatment for 1 min, no equilibration
4	MLT-MN 2 min	Maltose microneedle treatment for 2 min, no equilibration
5	MLT-MN 4 min	Maltose microneedle treatment for 4 min, no equilibration
6	MLT-MN 30E	Maltose microneedle treatment for 1 min, 30-min equilibration
7	30E MLT-MN	Maltose microneedle treatment for 1 min, 30-min equilibration prior to the microneedle insertion
8	Admin 1200	Admin Pen™ 1200 treatment for 1 min, no equilibration
9	Admin 1500	Admin Pen™ 1500 treatment for 1 min, no equilibration

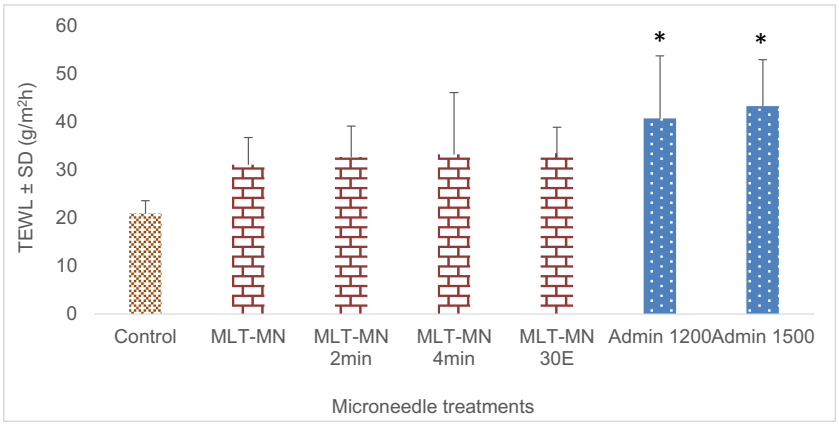

Fig. 10 Transepidermal water loss values of skin treated by different microneedles (*asterisks* indicate the statistical difference from control group)

In vitro permeation studies using vertical Franz diffusion cells

The effect of variation in needle length, equilibration time, and treatment duration on permeation of vismodegib was evaluated in vitro using dermatomed porcine ear skin. Skin that was neither pierced by microneedles nor equilibrated was selected as control. No vismodegib was expected to penetrate the skin when the passive diffusion experiments were performed [27]. The amount of vismodegib permeated across the skin treated with different methods was plotted as a function of time (n=4).

According to Fig. 11, maltose microneedle treatment (14.50±2.35 μg/cm^2) delivered a significantly smaller amount of drug to the receptor than Admin Pen™ 1200 (32.38± 3.33 μg/cm^2) (p=0.000) and Admin Pen™ 1500 (74.40± 15.86 μg/cm^2) (p=0.000). Also, significantly higher amount of drug permeated through the skin treated by Admin Pen™ 1500 than that by Admin Pen™ 1200 (p=0.002). This data was consistent with the study of Badran et al. that also showed an increase in drug delivery with an increase in needle length [11]. The difference in the permeation results of maltose microneedle (MLT-MN), Admin 1200, and Admin 1500 might be explained due to the difference in the length and density of needles and the depth and surface area of microchannels. In particular, Admin Pen™ 1500, being the longest among the three (1396±8.89 μm), produced the deepest channels in the skin (278±33.35 μm). Moreover, Admin Pen™ 1500 had the greatest average total surface area of microchannels and the lowest needle density (31 needles/cm^2) to avoid "bed of nails" effect. Most drug molecules permeated through micropores rather than through the skin surrounding the channels [22]. These characterization results rationally supported the highest amount of drug delivered through Admin Pen™ 1500 treatment. However, the possibility of pain and damage to the small blood capillaries resulting in bleeding with the use of longer microneedles exists, as they are most likely to reach the nerve fibers. Also, the greater surface area of channels may offer potential entry to bacteria or other foreign substances in the skin tissues [18]. In other experiments, the equilibration was performed before maltose microneedle treatment (30E MLT-MN) to compare with the group where the 30-min equilibration time was given after the microneedle insertion (MLT-MN 30E). The treatment methods of different groups are mentioned in Table 3. The in vitro permeation profiles of vismodegib in 30E MLT-MN, MLT-MN 30E, MLT-MN, control 30E, and control groups

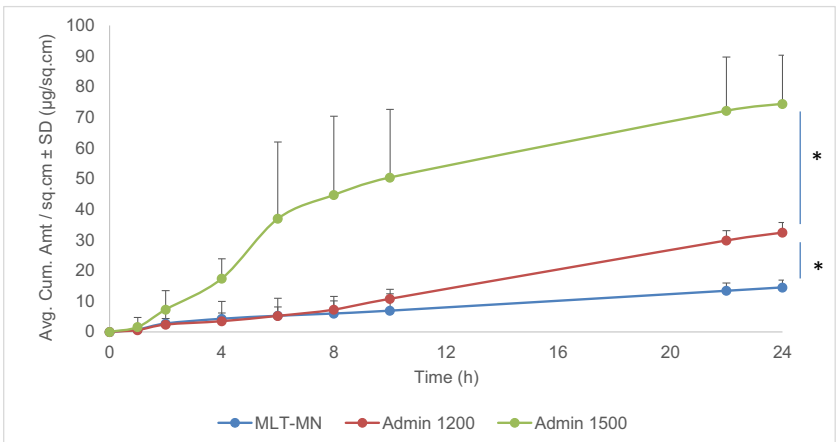

Fig. 11 In vitro permeation profile of vismodegib through microneedle-treated porcine ear skin: maltose microneedle, Admin Pen™ 1200, and Admin Pen™ 1500 (*asterisks* indicate the statistical difference between MLT-MN and Admin 1200 groups and between Admin 1200 and Admin 1500 groups)

were obtained from four replicates for each group. The results of cumulative amount of drug delivered per the diffusion area are illustrated in Fig. 12.

The enhanced delivery of vismodegib by maltose microneedle treatment was explained by the TEWL value measurement, dye binding, histology, and confocal microscopy studies that proved maltose microneedles pierced the stratum corneum and entered the dermis layer, thereby disturbing the skin barrier function. The similar result was obtained in the research of Kolli and Banga where solid maltose microneedles significantly increased the delivery of nicardipine hydrochloride through hairless rat skin in vitro and in vivo [5]. Besides, the magnitude of enhancement varied according to the physicochemical properties of drug, viscoelasticity of skin, and microneedle treatment methods. Without maltose microneedle treatment, the equilibration did not affect the permeation profile of vismodegib considerably as no significant difference between control (0.00±0.00 μg/cm^2) and control 30E (1.31±1.22 μg/cm^2) groups was observed (p=0.076). Both the 30-min equilibration time before and after the microneedle insertion significantly increased the permeability of vismodegib as compared to MLT-MN group (p<0.05). Besides, the use of equilibration before maltose microneedle treatment (30E MLT-MN, 36.28±11.21 μg/cm^2) did not give statistically different drug delivery from the group where the skin tissues were equilibrated after the insertion (MLT-MN 30E, 31.92±14.00 μg/cm^2) (p=0.64).

The similar effects of equilibration time on drug transdermal permeability have been discussed in the literature where the delivery of Rhodamine B was enhanced by 1-h equilibration [23]. Our previous study using full-thickness porcine ear skin indicated that vismodegib mostly remained in the stratum corneum and negligible amount was delivered to the receptor chamber [27]. Therefore, the reduction of thickness of skin dermis layer by dermatoming did not enhance the amount of drug penetrated across the skin as found in the control group (0.00±0.00 μg/cm^2).

The effect of different maltose microneedle treatment durations (1, 2, and 4 min) on transdermal delivery of vismodegib was plotted in Fig. 13 (n=4). It was observed that an increase in the needle insertion time from 1 to 2 min resulted in an insignificant increase in the amount of drug delivered (p=0.054). However, there was significant enhancement in drug permeation when the treatment duration increased from 1 min (MLT-MN, 14.50±2.35 μg/cm^2) to 4 min (MLT-MN 4 min, 49.00±13.09 μg/cm^2) (p=0.002). Thus, the 4-min treatment duration delivered the greatest amount of drug among the groups (MLT-MN, MLT-MN 2 min, MLT-MN 4 min). The present study was supported by other projects where the permeability of galanthamine was enhanced by an increase in the insertion time. This has been explained by Li et al. that during shorter duration of treatment, the skin contracts rapidly and microchannels close shortly, thereby producing lower skin permeability. For longer treatment duration, the skin around the channels causes reversible plastic deformation, delays elasticity recovery, allows the channels to sustain longer, and causes significant increase in skin permeability [37].

Skin disposition studies

Tape stripping is a useful technique to investigate the amount of drug in the stratum corneum and underlying layers of the skin samples. Vismodegib was extracted from tapes and skin using 2 ml ethanol before being quantitatively analyzed using the gradient HPLC method. The amount of drug in the stratum corneum and dermatomed skin of MLT-MN, Admin 1200, and Admin 1500 groups is shown in Fig. 14 (n=4).

As shown in Fig. 14, there was an insignificant difference in the total amount of vismodegib retained in the skin samples

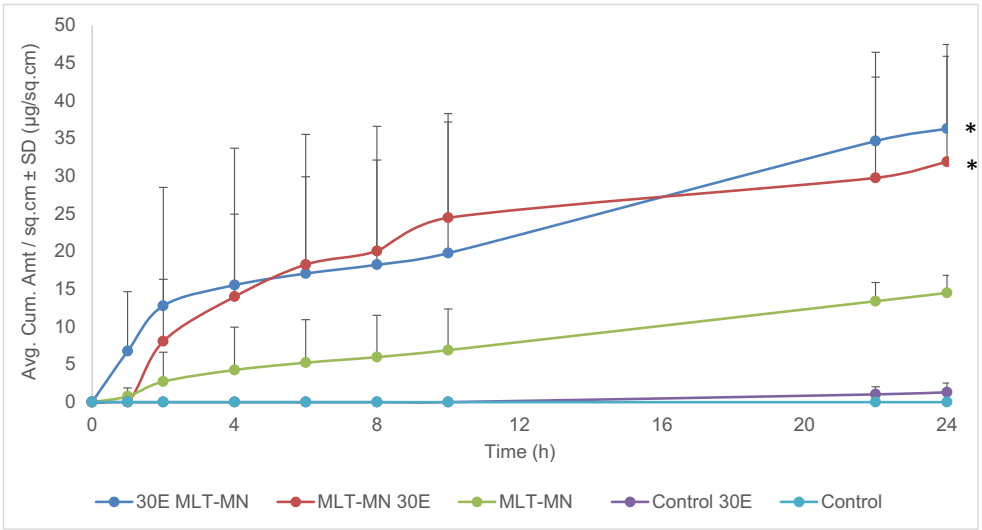

Fig. 12 In vitro permeation profile of vismodegib through microneedle-treated porcine ear skin: 30E MLT-MN, MLT-MN 30E, MLT-MN, control 30E, and control (*asterisks* indicate the statistical difference from MLT-MN group)

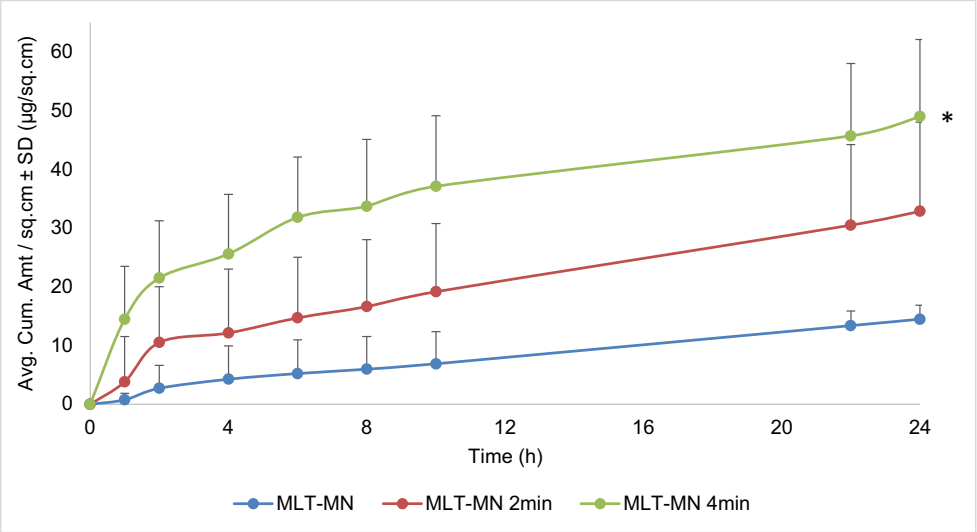

Fig. 13 In vitro permeation profile of vismodegib through microneedle-treated porcine ear skin: MLT-MN, MLT-MN 2 min, and MLT-MN 4 min (*asterisk* indicates the statistical difference between MLT-MN 4 min and MLT-MN group)

treated using different methods (MLT-MN, Admin 1200, and Admin 1500) ($p>0.05$). The drug level in the stratum corneum in MLT-MN group (24.16±3.40 µg/cm^2) was not significantly higher than that in Admin 1200 group (17.80±8.15 µg/cm^2) ($p=0.20$). However, Admin Pen™ 1500 produced a statistically lower level of vismodegib in the stratum corneum than maltose microneedles ($p=0.018$).

In order to investigate the effects of 30-min equilibration on the amount of drug in skin layers, skin samples harvested from in vitro permeation studies of control and control 30E groups ($n=4$) were analyzed for skin disposition data.

Figure 15 indicates that the amount of vismodegib in the stratum corneum layer in the two groups was not significantly different ($p=0.36$). However, the total amount of drug in the skin in control 30E group (57.69±20.14 µg/cm^2) was significantly higher than that in control group (24.51±7.85 µg/cm^2) ($p=0.022$). As shown in Fig. 12, an insignificant difference in the drug level in the receptor between control and control 30E groups was observed ($p=0.076$). Therefore, 30-min equilibration time was found to assist the drug entry into deeper skin layers. This finding may be explained due to the hydration of skin samples after the equilibration time.

Skin irritation test

An in vitro EpiDerm™ skin irritation test on the reconstructed human epidermal model EpiDerm (EPI-200-SIT) was conducted to investigate the irritancy level of vismodegib solution in PG (7 mg/ml). The results were plotted as means±SD ($n=3$) for drug formulation, positive control, and negative control in Fig. 16.

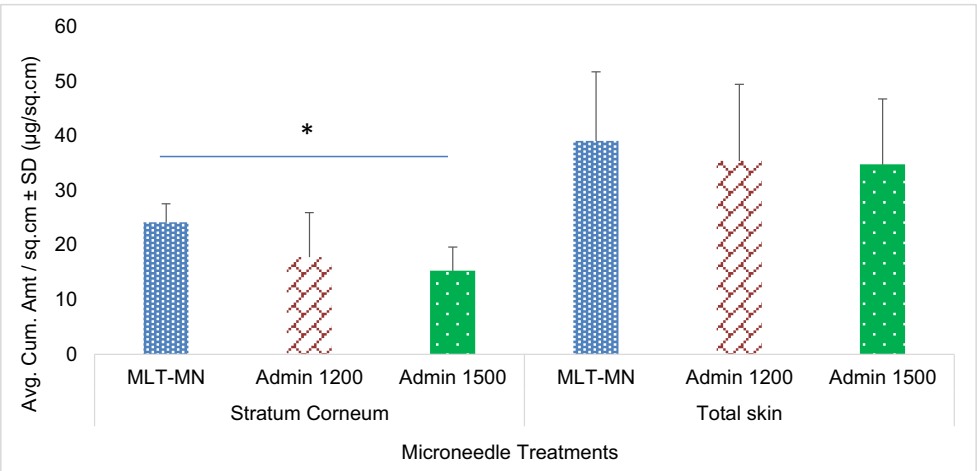

Fig. 14 The amount of vismodegib in skin layers: MLT-MN, Admin 1200, and Admin 1500 (*asterisk* indicates the statistical difference between MLT-MN and Admin 1500 groups)

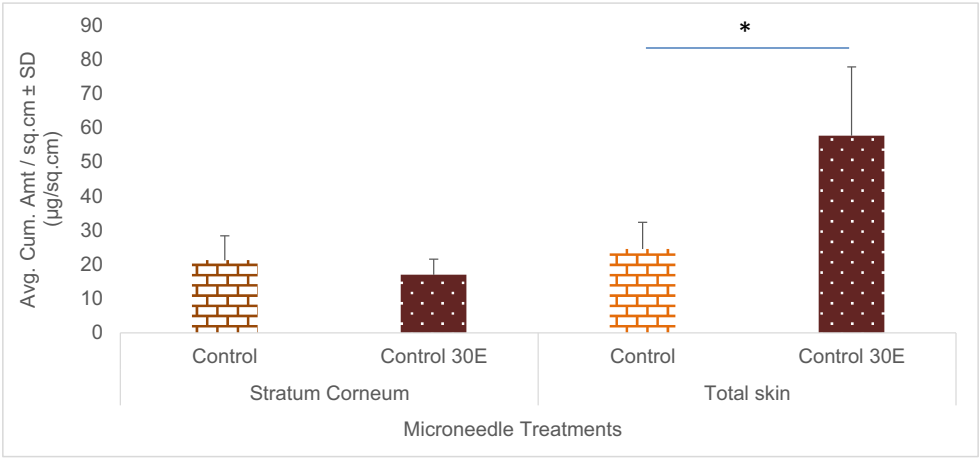

Fig. 15 The amount of vismodegib in skin layers: control and control 30E (*asterisk* indicates the statistical difference between the total amount of drug in the skin in control and control 30E groups)

As shown in Fig. 16, the mean viability of the negative control was 100.0±24.23 %, while that of the positive control was 3.3±0.56 %. The mean relative tissue viability of three individual tissues exposed to vismodegib formulation was 97.1±1.44 % that was greater than 50 %. The skin irritation test results showed that vismodegib solution in PG (7 mg/ml) was non-irritant (NI) to the reconstructed human epidermal model EpiDerm [29]. The experiment thus proved that vismodegib formulation could be applied safely on animal skin without any irritation [28].

Conclusion

The present study indicated that transdermal delivery of vismodegib across dermatomed porcine ear skin was enhanced by microneedle treatment. The difference in the in vitro drug permeation profile was affected by the needle length, equilibration time, and microneedle treatment duration. Scanning electron microscopy was utilized to characterize the geometry and dimensions of microneedles. Successful microporation of the skin samples was confirmed by dye binding and histology studies. Characterization of pore uniformity by calcein imaging showed that channels created by maltose microneedles were more uniform than those formed by Admin Pen™. In the in vitro permeation studies, the mean cumulative amount of drug permeated through the skin at 24 h by maltose microneedles was significantly lower than that by Admin Pen™ 1200 and Admin Pen™ 1500 ($p<0.05$). Equilibration time after microneedle treatment significantly increased the amount of vismodegib delivered to the receptor chamber ($p<0.05$). There was a positive correlation between the vismodegib transdermal delivery and the microneedle treatment duration. The amount of drug retained in skin layers was determined and compared between different treatment groups. In vitro irritation test on the reconstituted human epidermal model EpiDerm validated that vismodegib solution in propylene glycol (7 mg/ml) was non-irritant. The present study thus investigated the effect of needle length, equilibration time, and microneedle treatment duration on the delivery of vismodegib through dermatomed porcine ear skin.

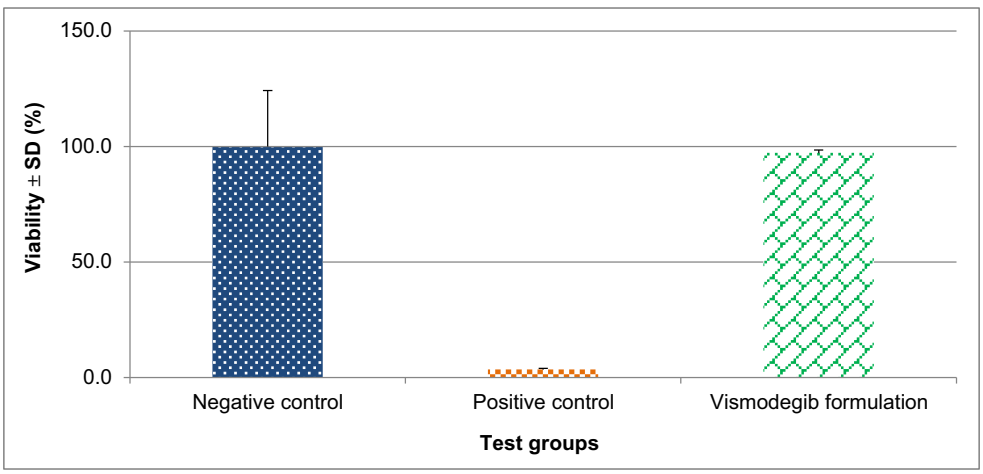

Fig. 16 The relative tissue viability in in vitro skin irritation test

Acknowledgments We are thankful to Ashana Puri, Department of Pharmaceutical Sciences, College of Pharmacy, Mercer University, for helping us to read the manuscript and provide helpful suggestions.

Conflict of interest The authors do not have any conflicts of interest to report for this manuscript.

References

1. Cowey CL. Targeted therapy for advanced basal-cell carcinoma: vismodegib and beyond. Dermatol Ther (Heidelb). 2013;3(1):17–31.
2. Macha MA, Batra SK, Ganti AK. Profile of vismodegib and its potential in the treatment of advanced basal cell carcinoma. Cancer Manag Res. 2013;5:197–203.
3. Fellner C. Vismodegib (Erivedge) for advanced basal cell carcinoma. PT. 2012;37(12):670–82.
4. Dancik Y, Anissimov YG, Jepps OG, Roberts MS. Convective transport of highly plasma protein bound drugs facilitates direct penetration into deep tissues after topical application. Br J Clin Pharmacol. 2012;73(4):564–78.
5. Kolli CS, Banga AK. Characterization of solid maltose microneedles and their use for transdermal delivery. Pharm Res. 2008;25(1):104–13.
6. Andrews SN, Jeong E, Prausnitz MR. Transdermal delivery of molecules is limited by full epidermis, not just stratum corneum. Pharm Res. 2013;30(4):1099–109.
7. Prausnitz MR, Langer R. Transdermal drug delivery. Nat Biotechnol. 2008;26(11):1261–68.
8. Mazlela T, Mahmood T, McCrudden MTC, Torrisi BM, McAlister E, Garland MJ, et al. Microneedles for intradermal and transdermal drug delivery. Eur J Pharm Sci. 2013;50(5):623–37.
9. Kim YC, Park JH, Prausnitz MR. Microneedles for drug and vaccine delivery. Adv Drug Deliv Rev. 2012;64(14):1547–68.
10. Bolognia JL, Jorizzo JL, Schaffer JV. Dermatology. Philadelphia: Elsevier Saunders; 2012.
11. Badran MM, Kuntsche J, Fahr A. Skin penetration enhancement by a microneedle device (Dermaroller) in vitro: dependency on needle size and applied formulation. Eur J Pharm Sci. 2009;36(4-5):511–23.
12. Hampton T. Breaking barriers in transdermal drug delivery. J Am Med Assoc. 2005;293:2083.
13. Williams AC, Barry BW. Penetration enhancers. Adv Drug Deliv Rev. 2004;56:603–18.
14. Coulman S, Allender C, Birchall J. Microneedles and other physical methods for overcoming the stratum corneum barrier for cutaneous gene therapy. Crit Rev Ther Drug Carrier Syst. 2006;23(3):205–58.
15. Arora A, Prausnitz MR, Mitragotri S. Micro-scale devices for transdermal drug delivery. Int J Pharm. 2008;364(2):227–36.
16. Li G, Badkar A, Kalluri H, Banga AK. Microchannels created by sugar and metal microneedles: characterization by microscopy, macromolecular flux and other techniques. J Pharm Sci. 2010;99(4):1931–41.
17. Yuzhakov VV. The AdminPen™ microneedle device for painless & convenient drug delivery. Drug Deliv Technol. 2010;10(4):32–6.
18. Donnelly RF, Singh TR, Tunney MM, Morrow DI, McCarron PA, O'Mahony C, et al. Microneedle arrays allow lower microbial penetration than hypodermic needles in vitro. Pharm Res. 2009;26(11):2513–22.
19. Kaur M, Ita KB, Popova IE, Parikh SJ, Bair DA. Microneedle-assisted delivery of verapamil hydrochloride and amlodipine besylate. Eur J Pharm Biopharm. 2014;86(2):284–91.
20. Gomaa YA, Morrow DIJ, Garland MJ, Donnelly RF, El-Khordagui LK, Meidan VM. Effects of microneedle length, density, insertion time and multiple applications on human skin barrier function: assessments by transepidermal water loss. Toxicol in Vitro. 2010;24(7):1971–8.
21. Cheung K, Han T, Das DB. Effect of force of microneedle insertion on the permeability of insulin in skin. J Diabetes Sci Technol. 2014;8(3):444–52.
22. Milewski M, Yerramreddy TR, Ghosh P, Crooks PA, Stinchcomb AL. In vitro permeation of a pegylated naltrexone prodrug across microneedle-treated skin. J Control Release. 2010;146(1):37–44.
23. Gomaa YA, El-Khordagui LK, Garland MJ, Donnelly RF, McInnes F, Meidan VM. Effect of microneedle treatment on the skin permeation of a nanoencapsulated dye. J Pharm Pharmacol. 2012;64(11):1592–602.
24. AdminPen Devices. http://adminmed.com/adminpen. Accessed 11 Sep 2014.
25. Han T, Das DB. Permeability enhancement for transdermal delivery of large molecule using low-frequency sonophoresis combined with microneedles. J Pharm Sci. 2013;102(10):3614–22.
26. Olatunji O, Das DB, Garland MJ, Belaid L, Donnelly RF. Influence of array interspacing on the force required for successful microneedle skin penetration: theoretical and practical approaches. J Pharm Sci. 2013;102(4):1209–21.
27. Nguyen HX, Banga AK. Determination of vismodegib by gradient reverse-phase high-performance liquid chromatography. Int J Pharmaceut Anal. 2014. In press.
28. MatTek Corporation (2009) Protocol for: in vitro EpiDerm™ skin irritation test (EPI-200-SIT) for use with MatTek Corporation's reconstructed human epidermal model EpiDerm (EPI-200). MatTek Corporation (Ashland, MA, USA)
29. Kandárová H, Hayden P, Klausner M, Kubilus J, Sheasgreen J. An in vitro skin irritation test (SIT) using the EpiDerm reconstructed human epidermal (RHE) model. J Vis Exp. 2009;29:1366.
30. Zhang D, Das DB, Rielly CD. Microneedle assisted micro-particle delivery from gene guns: experiments using skin-mimicking agarose gel. J Pharm Sci. 2014;103(2):613–27.
31. Pig ear skin. http://zyleris.com/faq.php. Accessed 11 Sep 2014.
32. Gupta J, Gill HS, Andrews SN, Prausnitz MR. Kinetics of skin resealing after insertion of microneedles in human subjects. J Control Release. 2011;154:148–55.
33. Martanto W, Moore JS, Couse T, Prausnitz MR. Mechanism of fluid infusion during microneedle insertion and retraction. J Control Release. 2006;112(3):357–61.
34. Yan G, Warner KS, Zhang J, Sharma S, Gale BK. Evaluation needle length and density of microneedle arrays in the pretreatment of skin for transdermal drug delivery. Int J Pharm. 2010;391(1-2):7–12.
35. Verbaan FJ, Bal SM, van den Berg DJ, Groenink WH, Verpoorten H, Lüttge R, et al. Assembled microneedle arrays enhance the transport of compounds varying over a large range of molecular weight across human dermatomed skin. J Control Release. 2007;117(2):238–45.
36. Elmahjoubi E, Frum Y, Eccleston GM, Wilkinson SC, Meidan VM. Transepidermal water loss for probing full-thickness skin barrier function: correlation with tritiated water flux, sensitivity to punctures and diverse surfactant exposures. Toxicol In Vitro. 2009;23(7):1429–35.
37. Li WZ, Huo MR, Zhou JP, Zhou YQ, Hao BH, Liu T, et al. Super-short solid silicon microneedles for transdermal drug delivery applications. Int J Pharm. 2010;389(1-2):122–9.